Pharm Res (2014) 31:1566–1574
DOI 10.1007/s11095-013-1262-6

RESEARCH PAPER

Comparative Studies on the Influences of Primary Emulsion Preparation on Properties of Uniform-Sized Exenatide-Loaded PLGA Microspheres

Feng Qi • Jie Wu • Dongxia Hao • Tingyuan Yang • Yu Ren • Guanghui Ma • Zhiguo Su

Received: 16 July 2013 / Accepted: 9 December 2013 / Published online: 8 January 2014

ABSTRACT

Purpose It is well known that primary emulsion (W_1/O) preparation process (by ultrasonication or homogenization) plays an important role in the properties of drug-loaded microspheres, such as encapsulation efficiency, release behavior and pharmacodynamics. However, its involved mechanism has not been intensively and systematically studied, partly because that broad size distribution of the resultant particles prepared by conventional preparation can greatly disturb the analysis and reliability of the results. Here, we focused on the relevant studies.

Methods In order to eliminate the disturbance caused by broad size distribution, uniform-sized exenatide-loaded poly(DL-lactic-co-glycolic acid) (PLGA) microspheres were prepared by Shirasu Porous Glass (SPG) premix membrane emulsification. The properties of microspheres whose W_1/O was formed by ultrasonication (UMS) and homogenization (HMS) were compared including *in vitro* release, pharmacology and so forth.

Results HMS exhibited fast release rate and hyperglycemic efficacy within first 14 days, but declined afterwards. Comparatively, UMS showed slower polymer degradation, more acidic microclimate pH (μpH) *in vitro*, and stable drug release with sustained efficacy during 1 month *in vivo*.

Conclusions HMS was desirable for the 2-week-sustained release *in vivo*, while UMS was more appropriate for the longer time release (about 1 month). These comparative researches can provide guidance for emulsion-microsphere preparation routs in pharmaceutics.

F. Qi • J. Wu • D. Hao • T. Yang • Y. Ren • G. Ma (✉) • Z. Su
National Key Laboratory of Biochemical Engineering,
PLA Key Laboratory of Biopharmaceutical Production & Formulation Engineering, Institute of Process Engineering, Chinese Academy of Sciences, Beijing 100190, People's Republic of China
e-mail: ghma@home.ipe.ac.cn

F. Qi
University of Chinese Academy of Sciences, Beijing 100049
People's Republic of China

KEY WORDS controlled release · homogenization · primary emulsion · ultrasonication · uniform-sized

INTRODUCTION

Water-oil–water ($W_1/O/W_2$) double emulsion method has been widely used to encapsulate hydrophilic drugs into microspheres. During the double emulsion formation, primary emulsion (W_1/O) preparation process has been demonstrated an important factor in the properties of microspheres, such as encapsulation efficiency, release behavior, and thus the drug efficacy (1–3). The W_1/O emulsion is generally formed by ultrasonication or homogenization (4–8), but their effects on the properties of resultant microspheres were seldom reported, and the involved mechanisms have not been clarified in detail. One difficulty to perform this study is the disturbance by the broad size distribution of the microspheres that are prepared by conventional mechanical stirring (1–3), because it will cause poor preparation reproducibility, release behavior, drug efficacy and so forth (9). Considering above, here we carry out an exhaustive study on the discrepancy of microspheres prepared by ultrasonication and homogenization, by utilizing Shirasu Porous Glass (SPG) premix membrane emulsification to control particle size and narrow down size distribution (10–13). Poly(DL-lactic-co-glycolic acid) (PLGA), one of the few polymers approved by the Food and Drug Administration (FDA) with good biodegradability and biocompatibility (14), was used as material. Exenatide, a therapy for type 2 diabetes mellitus (T2DM), possessing glucoregulatory function was selected as a model peptide. Uniform-sized exenatide-loaded PLGA microspheres were prepared by SPG premix membrane emulsification combined with $W_1/O/W_2$ double emulsion method.

In this study, microspheres whose W_1/O was respectively formed by ultrasonication (UMS) and homogenization (HMS) were compared including their morphological changes, dry

weight loss, molecular weight (M_w) degradation and so forth. The mechanisms of release and degradation were analyzed by observing variations of drug distribution and microclimate pH (μpH). Stability of exenatide during preparation, storage and *in vitro* release was determined. Pharmacokinetics and pharmacodynamics were also accessed to study their pharmacological actions *in vivo*.

MATERIALS AND METHODS

Materials

PLGA with mol ratio of D,L-lactide/glycolide 75/25 (M_w 13 kDa) was purchased from Lakeshore Biomaterials (Birmingham, AL, USA). Exenatide was provided by Hybio Pharmaceutical Co., Ltd. (Shenzhen, China). Poly(vinyl alcohol) (PVA-217, degree of polymerization 1,700, degree of hydrolysis 88.5%) was provided by Kuraray (Japan). SPG membranes were purchased from SPG Technology Co., Ltd. (Japan). The SPG premix membrane emulsification equipment (FMEM-500 M) was designed by National Engineering Research Center for Biotechnology (NERCB, Beijing, China). Acetonitrile and trifluoroacetic acid (TFA) (both in HPLC grade) were purchased from Dikma Co., Ltd. (USA). All other reagents were analytical grade.

Preparation of Microspheres

UMS and HMS were prepared by SPG premix membrane emulsification combined with $W_1/O/W_2$ double emulsion-solvent evaporation method. First, 1 mL exenatide aqueous solution (3%, w/v, W_1) was emulsified with 8 mL organic solvent (methylene dichloride, O) containing PLGA (10%, w/v) by ultrasonication (S-450D Digital Sonifier, Branson, USA) on 120 W or homogenization (T18, IKA, Germany) on 18,000 rpm for 60 s in ice bath to form W_1/O. Next, the W_1/O was mixed with external aqueous phase (W_2) containing PVA (2%, w/v) and NaCl (0.5%, w/v) to form coarse $W_1/O/W_2$ emulsions. Then they were poured into premix reservoir and extruded through the SPG membrane (50.2 μm) by N_2 pressure to achieve uniform-sized droplets. After that, they were solidified at room temperature for 5 h. Finally, the microspheres were collected by centrifugation, washed with distilled water for 5 times and obtained after freeze-drying.

Surface Morphology Observation and Size Distribution Measurement

The shape, surface and inner structure morphology of PLGA microspheres were observed by a JSM-6700 F (JEOL, Japan) scanning electron microscope (SEM).

The particle size distribution was measured by laser diffraction using Mastersizer 2000 (Malvern, UK). It was referred as Span value and calculated as follows:

$$\text{Span} = \frac{D_{v,90\%} - D_{v,10\%}}{D_{v,50\%}}$$

where $D_{v,90\%}$, $D_{v,50\%}$ and $D_{v,10\%}$ are volume size diameters at 90%, 50% and 10% of the cumulative volume, respectively. The smaller Span value indicates the narrower size distribution.

The droplet size and size polydispersity index (PDI) of W_1 droplets in W_1/O emulsion were determined by Zeta Sizer (Nanoseries, Malvern, UK).

Loading Efficiency (LE) and Encapsulation Efficiency (EE) Measurement

PLGA microspheres (5 mg) were dissolved in a mixed solution composed of 150 μL acetonitrile and 850 μL 0.01 M HCl. The concentration of exenatide was determined by a reversed phase HPLC (RP-HPLC) system at room temperature with a C18 (250×4.6 mm×5 μm, Syncronis, Thermo) chromatographic column. The chromatography was performed with a linear gradient elution from 20 to 60% acetonitrile in ultrapure water containing 0.1% TFA for 16 min. The flow rate was 1 mL/min, and the UV absorbance was set at 214 nm. The LE and EE of the microspheres were calculated by following equations:

$$\text{LE}(\%, \text{w/w}) = \frac{\text{Mass of drug in microspheres}}{\text{Mass of microspheres}} \times 100\%$$

$$\text{EE}(\%, \text{w/w}) = \frac{\text{Loading efficiency}}{\text{Theoretical loading efficiency}} \times 100\%$$

In Vitro Release and Polymer Degradation Studies

PLGA microspheres (10 mg) were incubated in 1 mL 10 mM phosphate buffer saline (PBS) medium (pH 7.4) under agitation at 37°C. Supernatants were periodically collected by centrifugation and replaced with fresh buffer of equal volume. The concentration of exenatide in the supernatant was determined by Micro BCA Protein Assay Kit. All the release experiments were done in triplicate.

For determining the dry weight and M_w of the microspheres during incubation, samples were collected after centrifugation and freeze-drying. The dry weight was directly

weighted, and the M_w was determined by gel permeation chromatography (GPC).

Observation of Drug Distribution and μpH Inside Microspheres

Super Fluor 488 SE (Fanbo Biochemicals, Beijing, China) was used to label exenatide to observe drug distribution within UMS and HMS during incubation. The microspheres preparation and *in vitro* release experiment were same as above. At predetermined times, a small amount of microspheres were removed from the samples and observed by confocal laser scanning microscopy (CLSM, Leica TCS SP 5) at exciting wave length 488 nm.

To monitor the μpH changes inside UMS and HMS, SNARF-1® dextran was added in W_1 (3~4 mg/mL). The probe was excited at 488 nm, and two images at different wavelengths (580 and 640 nm) were taken by CLSM. Then, the two images were overlapped to observe μpH change, and the ratio (I_{640}/I_{580}) variations with time were accessed. The fluorescence intensity became weaker and weaker since more amounts of probe were released from microspheres, so the images on the 100th day were not taken.

Animal Experiments and Statistics

Animal experiments were consistent with the guidelines set by the National Institutes of Health (NIH publication No. 85–23, revised 1985) and were approved by the Experimental Animal Ethics Committee in Beijing. The two experiments were performed in Beijing Dingguo changsheng Biotechnology Co., Ltd.

Male Sprague—Dawley (SD) rats (250~300 g) were used in the pharmacokinetics experiment. Eighteen rats were randomly divided into 3 groups (n=6 per group): exenatide solution group, UMS group and HMS group. Rats in the first group were received a single subcutaneous injection of exenatide solution at a dose of 36 μg/rat. Rats in the second group were received a single subcutaneous injection of a suspension of UMS at a dose of 1 mg/rat (equivalent to the dose of twice daily injection of exenatide solution for 2 weeks), so were those in HMS group. Plasma was separated *via* centrifugation and then stored at −70°C until assay. The exenatide concentration in plasma was analyzed by Exendin-4 EIA kit (Phoenix pharmaceuticals, CA, USA). The area under the concentration-time curve (AUC) was estimated by linear trapezoidal method, and the apparent elimination rate constant (K_{el}) was calculated by the least-squares regression analysis. The cumulative release *in vivo* was evaluated as follows:

$$\text{Cumulative release } in\ vivo = \frac{AUC_{0\sim t}}{AUC_{0\sim 30d} + C_{30d}/K_{el}} \quad (1)$$

The *in vitro-in vivo* correlations for UMS and HMS were established according to the cumulative release *in vitro* and *in vivo*.

Male db/db mice (6~7 weeks old) were used in the pharmacodynamics study. They were assigned into four groups randomly (n=6 per group): exenatide solution group, UMS group, HMS group and saline group. The mice in exenatide solution group were injected subcutaneously twice daily for 14 days (30 μg/kg). Mice in UMS and HMS group were received a single subcutaneous injection at first day (23 mg/kg for UMS and 25 mg/kg for HMS, both containing 0.84 mg/kg exenatide equivalent to total dose of exenatide solution for 2-week-twice daily injection). Those in saline group were also received a single subcutaneous injection at first day. One-touch blood glucose meter (ACCU-CHEK® Perfoma) was used to measure the non-fasting blood glucose.

The results of pharmacokinetics and pharmacodynamics were analyzed as means ± standard error (SE).

RESULTS AND DISCUSSION

Characteristics of UMS and HMS

Uniform-sized exenatide-loaded PLGA microspheres (UMS and HMS) were successfully prepared based on our previous optimization by SPG premix membrane emulsification (15). Both of them achieved high EE (Table I), and that of UMS was slightly higher. Their average particle sizes were around 20 μm with narrow size distribution (Fig. 1a), since the particle size and the size distribution were mainly influenced by membrane pore size and trans-membrane pressure (16), not by W_1/O preparation process. Their external surface morphologies were spherical and smooth with few pores (Fig. $1b_1$ and c_1). However, their inner structures were different (Fig. $1b_2$ and c_2) as that UMS had smaller pores in it with dense matrix and HMS exhibited larger pores with a relatively loose inner structure. Another difference was the exenatide distribution within microsphere evaluated by CLSM, in which the aqueous inner droplets containing drug were reflected by the green circles. As shown in Fig. $1b_3$, the drug droplets were distributed uniformly within matrix in UMS. In contrast, the

Table I Obtained Experimental Results of UMS and HMS (Results are Mean ± Standard Deviation (SD), n=3)

	Average particle size/μm	Span	EE/%	LE/%
UMS	21.85 ± 0.22	0.666	100.13 ± 1.89	3.65[a]
HMS	22.69 ± 0.13	0.678	91.81 ± 2.40	3.40 ± 0.11

[a] Owing to overestimation of EE, the actual LE was considered as theoretical LE

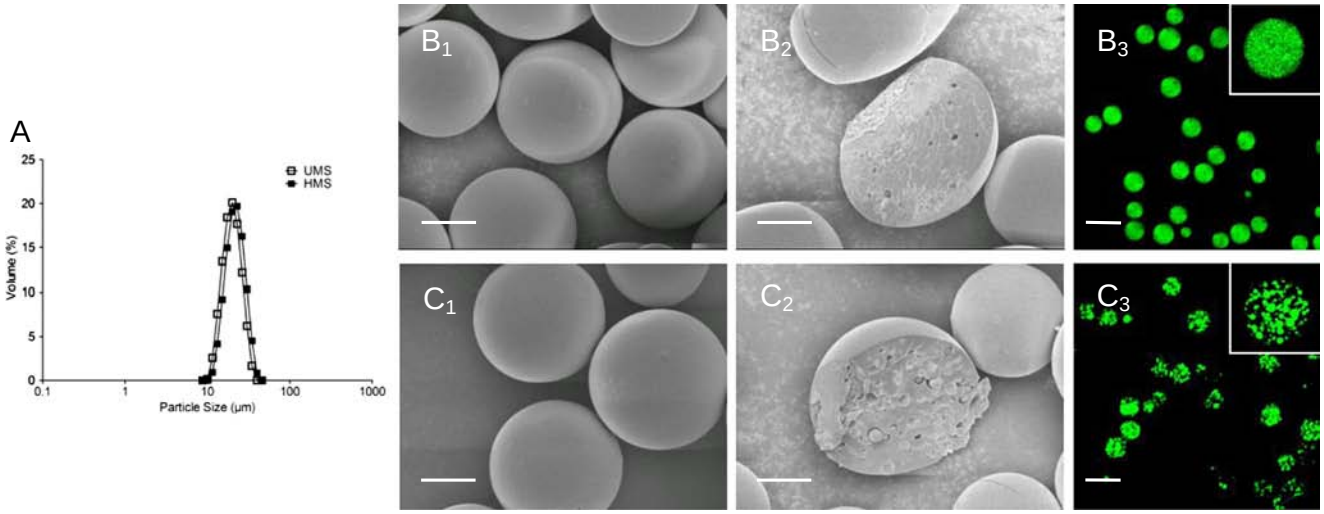

Fig. 1 (**a**) Size distributions of UMS and HMS; SEM images: surface morphology of (**b_1**) UMS and (**c_1**) HMS, crossing-section of (**b_2**) UMS and (**c_2**) HMS, scale bar: 10 μm. CLSM images: distribution of Super Fluor 488 SE labeled exenatide within (**b_3**) UMS and (**c_3**) HMS, scale bar: 50 μm.

droplets were distributed non-uniformly in HMS with much larger and inhomogenous aggregations (Fig. 1c_3).

These phenomena were attributed to the different operating principles of ultrasonication and homogenization. Ultrasonication caused droplets disruption in liquid-liquid system by cavitation (17). High shear force and large pressure caused by the cavitation could produce very fine uniform inner droplets (W_1) (308.07±7.00 nm, PDI: 0.078) that were distributed homogeneously in O phase to form W_1/O emulsion. After that, the emulsion was poured into W_2 phase, making the fine droplets distributed homogeneously in final particles. Small pores could thus be generated when the solidification was completed. Comparatively, homogenization broke the droplets by agitation with a relatively low shear force, resulting in production of larger non-uniform W_1 droplets (1242.77± 456.75 nm, PDI: 0.659) in the W_1/O emulsion. Consequently, large pores were formed in microspheres after solidification.

In Vitro Release

The cumulative release profiles *in vitro* of UMS and HMS were quite different (Fig. 2). HMS exhibited an initial burst release (about 25% within 24 h) followed by extended drug release over 40 days. However, its release rate leveled off afterwards until reached saturation (about 80%). Conversely, UMS presented a typical triphasic profile with an initial lower burst (about 13% within 24 h). In a long period up to 3 weeks, the release rate was slow, but then the release rate was increased. Finally, the saturation was achieved with uncompleted release (about 75%). To further investigate the mechanism, relevant experiments were undertaken as follows.

Polymer Degradation

Polymer degradation was evaluated by determination of particle dry weight and polymer M_w. As illustrated in Fig. 3a, up to the 3rd week, there was no difference between UMS and HMS. Afterwards, the mass loss of HMS started rapidly, because its loose inner structure caused more degraded PLGA oligomers and tight-binding drug molecules diffuse out of the matrix easily. Similarly, its decreasing rate of M_w also became faster than UMS at the same time (Fig. 3b). A possible explanation was that owing to the dense matrix of UMS, amounts of degraded oligomers were limited to diffuse into external media, giving rise to its local degradation within particles. Therefore, UMS was difficult to present significant mass loss and M_w decrease.

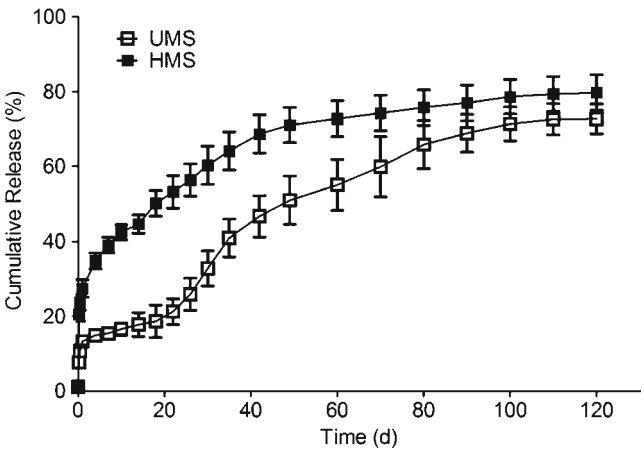

Fig. 2 Cumulative *in vitro* release profiles of UMS and HMS, data are mean ± SD ($n=3$).

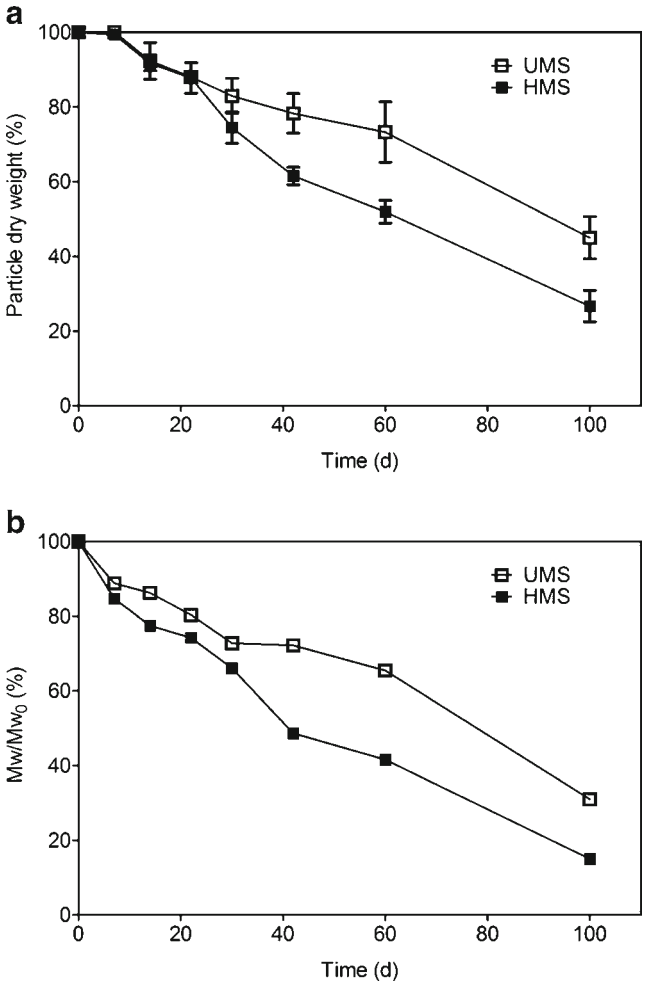

Fig. 3 (**a**) Particle dry weight (%, dry weight at each sampling time/initial dry weight) and (**b**) M_w/M_{w0} (%, M_w at each sampling time/initial M_{w0}) *vs.* time profiles of UMS and HMS.

Morphological and Inner Structural Changes

The states of microsphere degradation were also reflected by the morphological and inner structural changes. The morphological changes during *in vitro* release were shown in Fig. 4a. After 14-day incubation, both UMS and HMS remained intact, except for a bit of deformation. With incubation proceeding, pores began to form and gradually increased on their surfaces. Surprisingly, both of them still maintained their integrities up to 60 days. It was because that the reduced glass transition temperature (T_g), arose from the decreased M_w, promoted the mobility of degraded polymer oligomers and accelerated their aggregation by plasticization (18). Therefore, the collapse of microspheres did not occur even up to 100 days. In the end, it was obviously that the particles became smaller, and some were aggregated with coarse surface. Moreover, the maintaining integrity might be one of the reasons for the uncompleted release.

The inner structural changes that could affect the *in vitro* release behavior (19,20) were reflected by the drug distribution variations visualized *via* CLSM. As evidently indicated in Fig. 4b, the inner structure of UMS was still relatively dense, leading to slow release within first 14 days. During this period, the hydrophilic peptide molecules migrated from drug domains toward exterior of the microspheres and diffused throughout the polymer matrix. Simultaneously, the drug domains changed into aqueous pores (3,21), and with incubation proceeding, the pores became larger and larger (30 and 60 days). It may be attributed that the dense inner structure of UMS limited the diffusion of polymer oligomers into external phase, and then local degradation was accelerated along with accumulation of more oligomers (22). Meanwhile, the cumulating oligomers promoted further local degradation in turn to form large pores within UMS. These phenomena also verified the conjecture discussed above, that is, M_w of the polymer in UMS was not significantly decreased because of the local degradation (Fig. 3b). As for HMS, owing to its loose inner structure, more pores were generated and contacted with external phase. Thus, no matter water or the degraded oligomers could diffuse into and out of the matrix easily. This is why its cumulative release and decreasing rate of M_w were both higher than UMS.

μpH Within Microspheres

The μpH within PLGA microspheres can readily develop into acidity due to the polymer degradation (23). Herein, aiming for a deeper insight into the degradation and the μpH inside microspheres over incubation, SNARF-1® dextran was encapsulated with exenatide and observed by CLSM. The emission spectrum of the fluorescent probe undergoes a pH-dependent wavelength shift. The dye shows red light (pH close to 6.0) and green light (pH close to 9.0), when the strongest fluorescence emission is near 580 and 640 nm. When the dye shows yellow, the pH is close to neutrality. Additionally, the ratio of the fluorescence intensities from the dye at two emission wavelengths (640 and 580 nm) is used to analyze μpH, and the lower value indicates the more acidic pH (24).

As demonstrated in Fig. 5a, UMS and HMS both presented yellow at first day, indicative of neutral pH. With incubation proceeding, they both turned into orange gradually, suggesting that the μpH became acid. For quantitative analysis of μpH changes, the ratios of fluorescence intensities measured at two wavelengths (I_{640}/I_{580}) were calculated at different incubation times. As shown in Fig. 5b, except the first day, UMS exhibited lower values (I_{640}/I_{580}) than HMS during the incubation, implying that the μpH inside UMS was more acidic. This result strongly supported the speculation again that the oligomers inside UMS were hard to diffuse out leading to more acidic μpH and local degradation. However, HMS began to recover to neutral pH at late stage (35 days to 60 days), because more small pores inside it (Fig. 4b) made the matrix of microspheres much easier to achieve the external

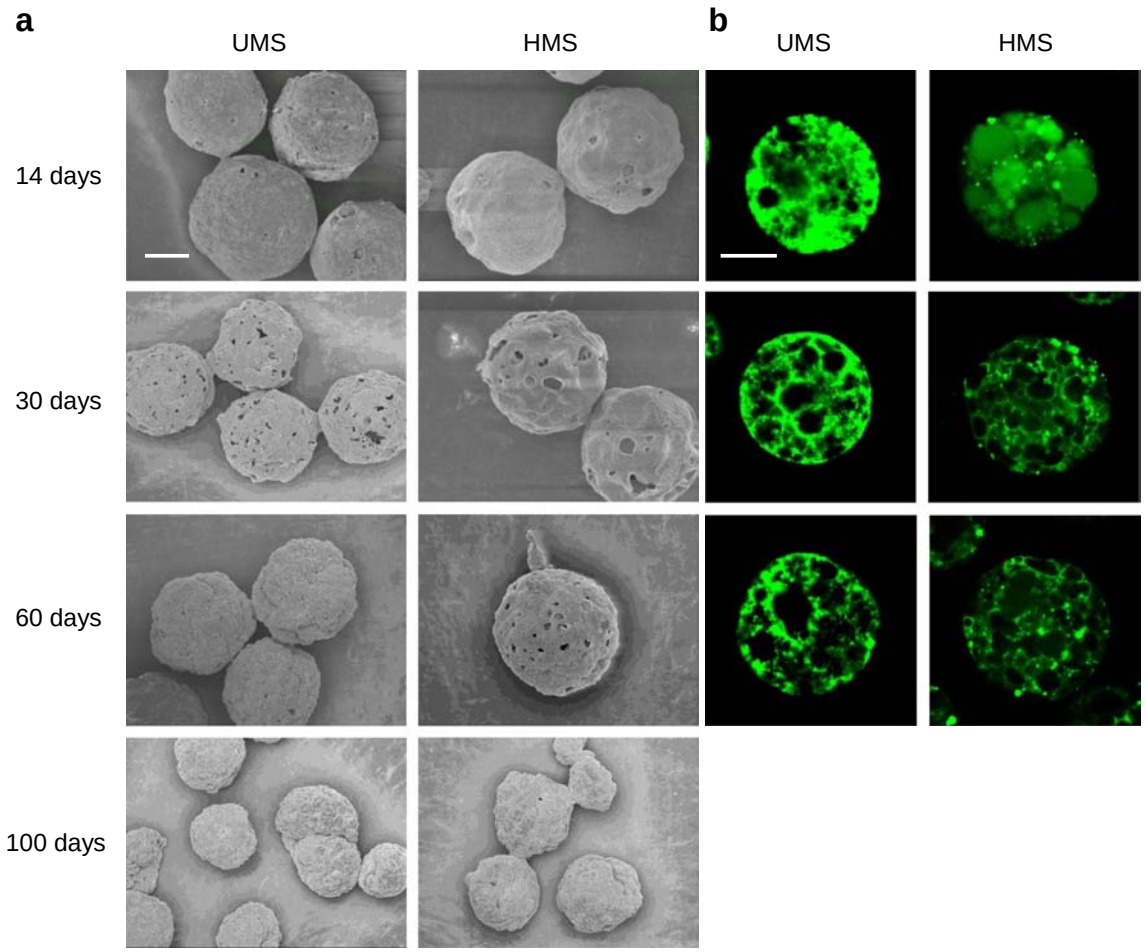

Fig. 4 (**a**) SEM images for morphological changes (*left panel*) and (**b**) CLSM images for inner structural changes (*right panel*) of UMS and HMS at different incubation times (14 days, 30 days, 60 days and 100 days), scale bar: 10 μm.

buffer. Meanwhile, UMS presented the same trend, although it was not that obvious.

Based on the above results, we found that the μpH inside UMS was acidic during the whole release period, but that inside HMS was in mild acidity and then back to neutrality. Whereas it is commonly known that continuous acidic environment is harmful for the stability of peptide or protein (25). Thus, we can draw a conclusion that drug-loaded microspheres prepared by ultrasonication are recommended to encapsulate the protein-protection agents to preserve the bio-stability of the drugs that are susceptible to acid; those prepared by homogenization are not necessary owing to short release period and mild μpH.

Stability

Stability of protein or peptide drugs in microspheres was readily influenced by the microenvironment inside microspheres such as pH, ionic strength, humidity and degraded polymer oligomers (25). With regard to exenatide, acylation that may affect the stability of the peptide easily occurred within PLGA microspheres (26), since the N-terminus and lysine side chain in the peptide were likely to interact with the polymer or its degraded oligomers (27). Therefore, the stability of exenatide during preparation as well as storage and release should be focused.

After freeze-drying, exenatide was extracted from UMS and HMS, and then detected by RP-HPLC and circular dichroism. Their spectrums were almost identical to the native one, indicating that the stability of the peptide was highly preserved during the preparation. Same detection were repeated after storage for 6, 12, 18 and 24 months at −20°C and 4°C, and similar results were obtained, indicating that the stability of the peptide was not affected either (data not shown).

However, during *in vitro* release, due to the high temperature (37°C), invasion of water and polymer degradation, the acylation would occur in UMS and HMS. Besides, this may be another reason for the uncompleted release.

Although the μpHs inside UMS and HMS were in acidity that might inhibit the acylation, the amounts of accumulated oligomers would still facilitate such reaction. Accordingly, the

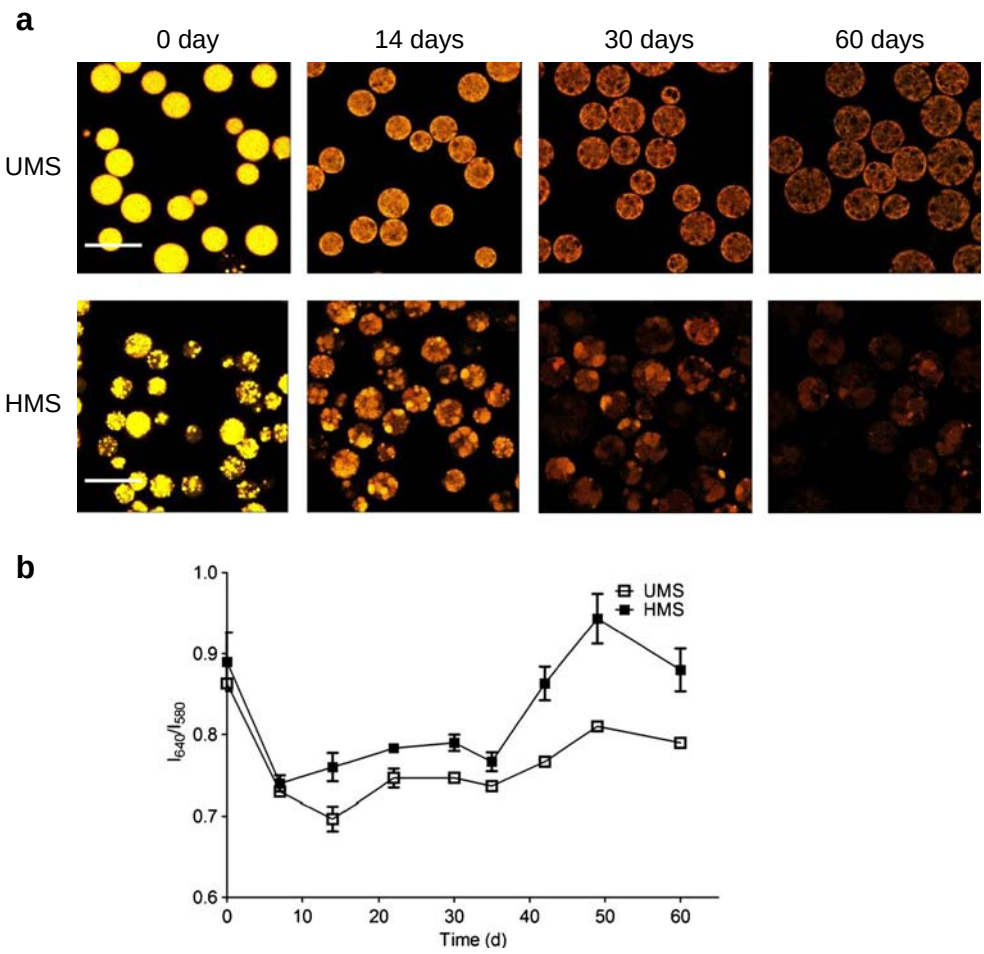

Fig. 5 (**a**) CLSM images of pH-sensitive dye-loaded UMS (*top panel*) and HMS (*bottom panel*) at different incubation times (0 day, 14 days, 30 days and 60 days), scale bar: 50 μm; (**b**) ratio of fluorescent intensity I_{640}/I_{580} *vs.* time profiles of UMS and HMS. Data are mean ± SD ($n=3$).

addition of additives seemed necessary to preserve the stability of exenatide. Therefore, how to keep the stability of exenatide during release will be further investigated by our team in the future.

Pharmacokinetics

Above studies focused on the comparison of physicochemical properties between UMS and HMS *in vitro*. However, due to the foreign body response, the situation *in vivo* was totally different from that *in vitro*. Thus, their pharmacology actions such as pharmacokinetics and pharmacodynamics should be further studied.

The pharmacokinetics of UMS and HMS were reflected by the plasma exenatide concentration for 30 days. After injection of corresponding formulations, all groups reached their maximum concentrations within 2 h as illustrated in Fig. 6a. The maximum value of HMS was higher than that of UMS due to its higher initial burst release. Simultaneously, they were both lower than the exenatide solution group. During the first 14 days, the plasma exenatide of HMS remained a higher level, and afterwards it became lower gradually until the end of 1 month. As for UMS, however, we interestingly found that the plasma drug level was almost constant within the whole period. Notably, it was higher than that of HMS in turn after 14 days.

In order to compare UMS and HMS more directly, their pharmacokinetic profiles were further represented in the calculated cumulative *in vivo* release in terms of Eq. (1) (Fig. 6b). To our surprise, the profile of HMS was similar to S-curve model within 1 month, whereas that of UMS presented as zero-order model. Note that the release rate of HMS became slower than UMS after 14 days, which was similar as the situation *in vitro* except the time (after 22 days *in vitro*). Apparently, the release behaviors *in vivo* were much slower than their counterparts *in vitro*. Because the biological compounds in body, such as enzymes, favored absorbing water into the microspheres or inducing foreign body response (28), the degradation of PLGA was accelerated leading to fast release.

The *in vitro-in vivo* correlations of UMS and HMS were established by the profiles of cumulative release *in vitro* and *in vivo* (Fig. 6c), exhibiting a good linear regression correlation. Based on this result, it was feasible to predict the release *in vivo* by the established correlation according to the release *in vitro*.

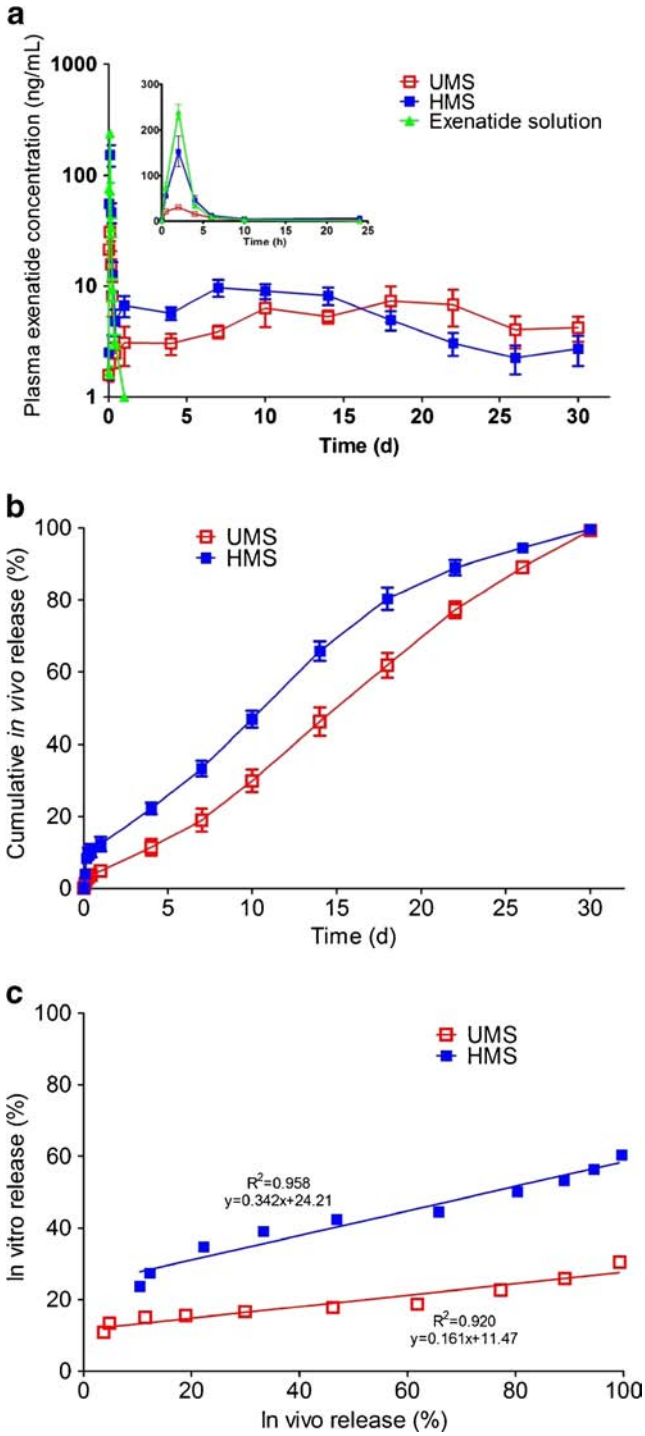

Fig. 6 (**a**) Plasma exenatide concentration *vs.* time profiles of UMS, HMS and exenatide solution, the insert presents the plasma exenatide concentrations *vs.* time within 24 h; (**b**) cumulative *in vivo* release of UMS and HMS calculated by Eq. (1), data are means ± SE ($n=6$); (**c**) *in vitro-in vivo* correlations for UMS and HMS.

Overall, the release of HMS was faster than UMS no matter *in vitro* or *in vivo* within first 2 weeks. Although they both exhibited sustained-release profiles, it was noteworthy that UMS presented a relatively stable release during longer period, indicating that it was a potential drug carrier in the long-effective release system for longer time.

Pharmacodynamics

Pharmacodynamics of UMS and HMS were examined with type 2 diabetic db/db mice by measuring blood glucose and compared with the negative control (saline group) and the exenatide solution group. To reduce individual differences, blood glucose values were represented as reduction in glucose (%) which was calculated as follows: (initial blood glucose-blood glucose)/initial blood glucose.

As shown in Fig. 7, UMS, HMS and the exenatide solution group all presented hypoglycemic efficacy compared with saline group. The blood glucose level of exenatide solution group was lowered down significantly within first 14 days. When the injection was stopped (at 14th day), the level began to rebound. Exhibiting the similar trend to this group, the blood glucose level in HMS group also decreased as amounts of exenatide were released during the first 14 days, but afterwards the efficacy got weaker gradually. As for UMS, it showed a stable hypoglycemic efficacy during 1 month, despite that the blood glucose level was slightly higher at early stage. These results were consistent with the above pharmacokinetics study.

According to the pharmacology studies, although UMS and HMS possessed similar drug loading, the pharmacological properties had their own characteristics. We interestingly found that HMS was desirable for 2-week-sustained release, while UMS was more appropriate for longer time, such as 1 month. These results were instructional for us to choose the desirable W_1/O emulsion formation method in preparation of microspheres. However, the stability of the peptide still remained an important issue that would be further studied.

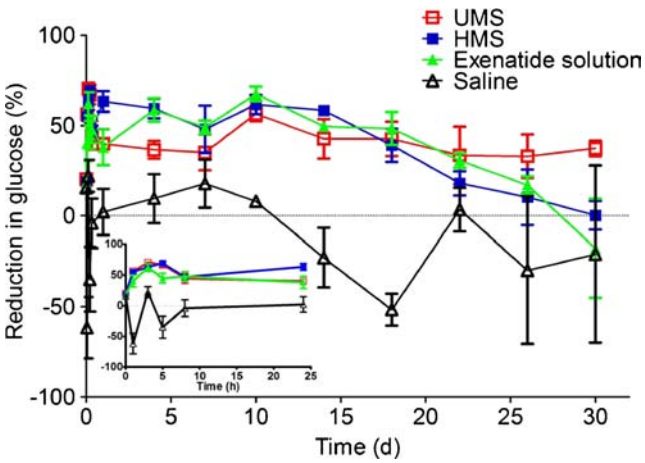

Fig. 7 Reduction in blood glucose *vs.* time profiles of UMS, HMS, exenatide solution and saline, the insert presents the reduction in blood glucose *vs.* time within 24 h. Data are mean ± SE ($n=6$).

CONCLUSION

In this study, uniform-sized exenatide-loaded UMS and HMS were prepared by SPG premix membrane emulsification. Comparative studies about their properties were performed intensively based on their high EE and same particle size with narrow size distribution. UMS presented relatively dense inner structure with slow release and degradation. Its μpH was almost acidic during the whole release period. However, pharmacological studies showed that it had the constant release and sustained efficacy during 1 month. Furthermore, due to the more acidic μpH inside UMS, protein-protection agents were recommended for preserving the bio-stability of drugs. In contrast, the inner structure of HMS was loose. Therefore, the release rate and degradation were faster, and the μpH was less acidic. Accordingly, it presented a faster release and a better efficacy within first 14 days *in vivo*. All these detailed comparative results can provide a renewed sense and guidance for emulsion-microsphere preparation or other long-effective release systems in pharmaceutics.

ACKNOWLEDGMENTS AND DISCLOSURES

Feng Qi and Jie Wu contributed equally to this work. We thank the Joint NSFC/RGC grant (21161160555) for the financial support provided.

REFERENCES

1. Mao SR, Xu J, Cai CF, *et al.* Effect of WOW process parameters on morphology and burst release of FITC-dextran loaded PLGA microspheres. Int J Pharm. 2007;334(1–2):137–48.
2. Sah HK, Toddywala R, Chien YW. Biodegradable microcapsules prepared by a W/O/W technique —effects of shear force to make a primary W/O emulsion on their morphology and protein release. J Microencapsul. 1995;12(1):59–69.
3. Yan CH, Resau JH, Hewetson J, *et al.* Characterization and morphological analysis of protein-loaded poly(lactide-co-glycolide) microparticles prepared by water-in oil-in-water emulsion technique. J Control Release. 1994;32(3):231–41.
4. Blanco D, Alonso MJ. Protein encapsulation and release from poly(lactide-co-glycolide) microspheres: effect of the protein and polymer properties and of the co-encapsulation of surfactants. Eur J Pharm Biopharm. 1998;45(3):285–94.
5. van de Weert M, Hoechstetter J, Hennink WE, *et al.* The effect of a water/organic solvent interface on the structural stability of lysozyme. J Control Release. 2000;68(3):351–9.
6. Morlock M, Koll H, Winter G, *et al.* Microencapsulation of rh-erythropoietin, using biodegradable poly(D, L-lactide-co-glycolide): protein stability and the effects of stabilizing excipients. Eur J Pharm Biopharm. 1997;43(1):29–36.
7. Zambaux MF, Bonneaux F, Gref R, *et al.* Preparation and characterization of protein C-loaded PLA nanoparticles. J Control Release. 1999;60(2–3):179–88.
8. Cai CF, Mao SR, Germershaus O, *et al.* Influence of morphology and drug distribution on the release process of FITC-dextran-loaded microspheres prepared with different types of PLGA. J Microencapsul. 2009;26(4):334–45.
9. Wang LY, Gu YH, Zhou QZ, *et al.* Preparation and characterization of uniform-sized chitosan microspheres containing insulin by membrane emulsification and a two-step solidification process. Colloids Surf, B. 2006;50(2):126–35.
10. Liu R, Ma G, Meng F, *et al.* Preparation of uniform-sized PLA microcapsules by combining Shirasu Porous Glass membrane emulsification technique and multiple emulsion-solvent evaporation method. J Control Release. 2005;103(1):31–43.
11. Liu R, Ma GH, Wan YH, *et al.* Influence of process parameters on the size distribution of PLA microcapsules prepared by combining membrane emulsification technique and double emulsion-solvent evaporation method. Colloids Surf, B. 2005;45(3–4):144–53.
12. Liu R, Huang SS, Wan YH, *et al.* Preparation of insulin-loaded PLA/PLGA microcapsules by a novel membrane emulsification method and its release in vitro. Colloids Surf, B. 2006;51(1):30–8.
13. Wei Q, Wei W, Tian R, *et al.* Preparation of uniform-sized PELA microspheres with high encapsulation efficiency of antigen by premix membrane emulsification. J Colloid Interf Sci. 2008;323(2):267–73.
14. Ahn JH, Park EJ, Lee HS, *et al.* Reversible blocking of amino groups of octreotide for the inhibition of formation of acylated peptide impurities in poly(lactide-co-glycolide) delivery systems. Aaps Pharmscitech. 2011;12(4):1220–6.
15. Qi F, Wu J, Fan Q, *et al.* Preparation of uniform-sized exenatide-loaded PLGA microspheres as long-effective release system with high encapsulation efficiency and bio-stability. Colloids Surf, B. 2013;112:492–8.
16. Wei Y, Wang Y, Wang L, *et al.* Fabrication strategy for amphiphilic microcapsules with narrow size distribution by premix membrane emulsification. Colloids Surf, B. 2011;87(2):399–408.
17. Priego-Capote F, de Castro L. Analytical uses of ultrasound - I. Sample preparation. Trac-Trend Anal Chem. 2004;23(9):644–53.
18. Wei GB, Pettway GJ, McCauley LK, *et al.* The release profiles and bioactivity of parathyroid hormone from poly(lactic-co-glycolic acid) microspheres. Biomaterials. 2004;25(2):345–52.
19. Yang YY, Chung TS, Bai XL, *et al.* Effect of preparation conditions on morphology and release profiles of biodegradable polymeric microspheres containing protein fabricated by double-emulsion method. Chem Eng Sci. 2000;55(12):2223–36.
20. Freiberg S, Zhu X. Polymer microspheres for controlled drug release. Int J Pharm. 2004;282(1–2):1–18.
21. Yushu H, Venkatraman S. The effect of process variables on the morphology and release characteristics of protein-loaded PLGA particles. J Appl Polym Sci. 2006;101(5):3053–61.
22. Ding AG, Schwendeman SP. Acidic microclimate pH distribution in PLGA microspheres monitored by confocal laser scanning microscopy. Pharm Res. 2008;25(9):2041–52.
23. Liu YJ, Schwendeman SP. Mapping microclimate pH distribution inside protein-Encapsulated PLGA microspheres using confocal laser scanning microscopy. Mol Pharmaceut. 2012;9(5):1342–50.
24. Li L, Schwendeman SP. Mapping neutral microclimate pH in PLGA microspheres. J Control Release. 2005;101(1–3):163–73.
25. Venier-Julienne MC, Giteau A, Aubert-Pouessel A, *et al.* How to achieve sustained and complete protein release from PLGA-based microparticles? Int J Pharm. 2008;350(1–2):14–26.
26. Liang R, Li X, Shi Y, *et al.* Effect of water on exenatide acylation in poly(lactide-co-glycolide) microspheres. Int J Pharm. 2013;454(1):344–53.
27. Schwendeman SP, Sophocleous AM, Zhang Y. A new class of inhibitors of peptide sorption and acylation in PLGA. J Control Release. 2009;137(3–4):179–84.
28. Tracy MA, Ward KL, Firouzabadian L, *et al.* Factors affecting the degradation rate of poly(lactide-co-glycolide) microspheres in vivo and in vitro. Biomaterials. 1999;20(11):1057–62.